Transverse current and generalized shear viscosity in liquid rubidium

U. Balucani and R. Vallauri
Istituto di Elettronica Quantistica del Consiglio Nazionale delle Ricerche, I-50127 Florence, Italy

T. Gaskell
Department of Physics, University of Sheffield, Sheffield S3 7RH, United Kingdom
(Received 13 January 1987)

The transverse current correlation function is studied in liquid rubidium by computer simulation, and the associated memory function is directly determined from the data, for a number of wave vectors. The usual phenomenological relaxation-time approximations for the memory function are shown to be inadequate, particularly in the wave-vector range where well-defined shear waves are supported by the liquid. A comparison of the results with new data obtained for a Lennard-Jones system is also made, and the dynamical processes contributing to the structure of the memory functions are assessed. The related generalized wave-vector-dependent shear viscosity, $\eta(q)$, is derived and its importance to the applicability of a microscopic Stokes-Einstein relation finally discussed. It is shown that the details in $\eta(q)$, which are revealed by the molecular-dynamics data, play a vital role in establishing this relation in liquid rubidium.

I. INTRODUCTION

A fundamental problem which most studies of dynamical properties of liquids try to clarify is the transition between the hydrodynamic and the microscopic regimes. In recent years important progress in this direction has been made, for instance by kinetic and mode-coupling theories,[1] or by approaches extending the concept of velocity field down to microscopic distances.[2,3] Away from the strict hydrodynamic regime, all the relevant memory functions show an increasingly "non-Markovian" behavior, conventionally described in terms of wave-vector and frequency-dependent transport coefficients. Remarkably enough, it is often found that several results obtained by pure hydrodynamic arguments maintain a validity in a much broader domain. The typical example is the Stokes-Einstein law for the diffusion coefficient, which can be derived microscopically, the only essential change being that the shear viscosity η is replaced by a generalized wave-vector-dependent viscosity $\eta(q)$.[4] In other circumstances even a formal extension is more complicated, and one is forced to adopt semiphenomenological models or simple prescriptions interpolating between the two regimes. In either case, computer simulation data have provided the traditional test for the theoretical results, as well as the guidance for more refined approaches.

One of the purposes of the present paper is to report molecular-dynamics (MD) data for $\eta(q)$ in a model system simulating liquid rubidium. As discussed in detail in the following, some general features of this generalized transport coefficient are found to be similar to those already reported for hard spheres[5] and for a Lennard-Jones (LJ) liquid.[6] As we shall see, in the case of liquid Rb, the discrepancies with respect to the simplest theoretical models (e.g., the viscoelastic one) are found to be much more important. Another reason of interest is the recent appearance of data for the wave-vector-dependent *longitudinal* viscosity [a quantity also involving $\eta(q)$], deduced from the results of *real* experiments in three liquid metals (Pb, Bi, Rb).[7]

The theoretical time-dependent quantity directly related to $\eta(q)$ is the memory function $n_T(q,t)$ associated with the transverse current, $\eta(q)$ essentially being the time integral of $n_T(q,t)$. Thus it seems worthwhile to explore also the dynamical features of the latter quantity in an extensive wave-vector interval, in particular in the "interesting" range where the system is able to support well-defined shear waves. In this work such an analysis is performed both in the liquid metal and in the LJ system, in order to emphasize the relevant differences in their dynamical behaviors. Moreover, the extent of validity of the commonly adopted phenomenological *ansätze*—which assume a decay of $n_T(q,t)$ with one or more relaxation times—can be established in both cases.

The detailed format of the paper is as follows. In Sec. II we review the properties of the generalized viscosity coefficient $\eta(q)$, including its determination from the transverse current correlation function $C_T(q,t)$. In Sec. III, after a short discussion of our simulation experiments, data for $C_T(q,t)$ are reported at several wave vectors. In Sec. IV we discuss the various numerical techniques by which it is possible to determine the associated memory function $n_T(q,t)$. Results for the latter are shown and the limitations of the simple phenomenological models are pointed out. Finally, in Sec. V we report the results obtained for $\eta(q)$ and discuss their consequences for the above-mentioned generalization of the Stokes-Einstein law.

II. RELEVANT PHYSICAL QUANTITIES

The shear viscosity coefficient η is the simplest transport property connected with the collective behavior of the system. The associated dynamical quantity is the

transverse current correlation function

$$C_T(q,t)=\left\langle \sum_i v_i^x(0)e^{-iqz_i(0)} \sum_j v_j^x(t)e^{iqz_j(t)} \right\rangle , \quad (1)$$

where the wave vector $\mathbf{q}$ is taken along the z axis. In the hydrodynamic limit one indeed finds that

$$[C_T(q,t)]_{\text{hydr}}=C_T(q,0)\exp[-(\eta q^2/\rho m)t] , \quad (2)$$

where $\rho=N/V$ is the number density and m is the atomic mass. In the following we shall frequently consider the normalized quantity $\rho_T(q,t)=C_T(q,t)/C_T(q,0)$ with $C_T(q,0)=Nk_BT/m$. Equation (2) is expected to be valid in a physical situation where the length and time scales are distinctly larger than the ones associated with "microscopic" processes involving the average range and duration of an atomic collision. When such conditions are not satisfied the monotonous decay implied by Eq. (2) is not valid, and the system is expected to support shear-wave propagation. On the other hand, this solidlike behavior gives rise to well-defined oscillations of $C_T(q,t)$ only in a limited range of wave vectors: As q becomes much larger than the inverse mean free path, the particles can be considered essentially free, thus yielding a purely kinetic Gaussian decay, $C_T(q,t)=C_T(q,0)\exp[-(k_BT/2m)q^2t^2]$, where every trace of collective behavior is lost.

The most convenient theoretical framework by which all these features can be interpreted is the memory-function formalism. In terms of Laplace transforms defined as

$$\hat{f}(z)=\mathscr{L}f(t)=\int_0^\infty dt\exp(-zt)f(t) ,$$

one finds that

$$\hat{\rho}_T(q,z)=[z+\hat{K}_T(q,z)]^{-1}=[z+(q^2/\rho m)\hat{\eta}(q,z)]^{-1} , \quad (3)$$

where $K_T(q,t)=\mathscr{L}^{-1}\hat{K}_T(q,z)$ is the transverse current memory function, whose initial value is given by

$$K_T(q,t=0)=\frac{q^2}{\rho m}\left[\rho k_BT+\frac{\rho^2}{q^2}\int d\mathbf{r}\,\frac{\partial^2\varphi(r)}{\partial x^2}(1-e^{-iqz})g(r)\right] . \quad (4)$$

Here the quantity in large parentheses defines the wave-vector-dependent rigidity modulus $G(q)$, expressed in terms of the pair potential $\varphi(r)$ and the pair distribution function $g(r)$. At liquid densities an excellent approximation for $G(q)$ is

$$G(q)=\rho k_BT+(\rho m\omega_E^2/q^2)[1-3j_1(q\sigma)/q\sigma] , \quad (4')$$

where ω_E is the Einstein frequency ($\omega_E=0.61\times10^{13}$ s^{-1} in liquid Rb at the temperature and density of our computer simulation study) and

$$j_1(x)=(1/x)[\sin(x)/x-\cos(x)]$$

is the $n=1$ spherical Bessel function. In the following we shall again find it convenient to deal with the normalized memory function

$$n_T(q,t)=K_T(q,t)/(q^2/\rho m)G(q) . \quad (5)$$

In the last member of Eq. (3) we have introduced a generalized wave-vector and frequency-dependent viscosity, $\hat{\eta}(q,z)$, which in the hydrodynamic limit $q\to0$, $z\to0$ coincides with the ordinary viscosity coefficient η. Beyond this regime a somewhat simpler description of the nonhydrodynamic effects is provided by the quantity $\eta(q)=\hat{\eta}(q,z=0)$. By Eqs. (3) and (5) we have that

$$\eta(q)=G(q)\hat{n}_T(q,z=0)=G(q)\int_0^\infty dt\,n_T(q,t) . \quad (6)$$

For instance, if we assume that $n_T(q,t)$ decays exponentially with a time constant $\tau(q)$—the so-called "viscoelastic model"—we deduce that $\eta(q)=G(q)\tau(q)$.

An equivalent expression of the wave-vector-dependent viscosity $\eta(q)$ reads

$$\eta(q)=\frac{\rho m}{q^2}\left[\int_0^\infty dt\,\rho_T(q,t)\right]^{-1} . \quad (7)$$

Both Eqs. (6) and (7) will be used in the following for the determination of $\eta(q)$ from the simulation data. Clearly, the gross dynamical features of the transverse current—e.g., the presence of "shear excitations"— have an important effect on the value of $\eta(q)$. No rigorous result is known on this wave-vector dependence, except

$$\eta(q)\sim(2m\rho^2k_BT/\pi)^{1/2}q^{-1} \text{ as } q\to\infty , \quad (8)$$

which holds at the large wave vectors characteristic of the free-particle regime.

III. COMPUTER SIMULATION EXPERIMENT

Our simulation experiment is performed by considering $N=500$ "rubidium atoms" in a box of length $L=36.15$ Å. The particles are assumed to interact by the effective potential of Price *et al.*[8] at a reduced density $\rho^*=\rho\sigma^3=0.905$, the same used by Rahman.[9] As shown in the latter reference, this potential accounts remarkably well for the static and dynamic structure factors as measured in liquid rubidium by neutron scattering. Several characteristics of the Price potential, more or less common to most liquid metals, have been found relevant in establishing important differences in the dynamical behavior with respect to the conventional LJ systems. For example, the experimental observation of inelastic peaks in the dynamic structure factor at relatively high wave vectors has been traced back to a softer core and a less anharmonic well than those pertinent to the LJ case.[10] At our density, the usual potential parameters are found to be $\sigma=4.405$ Å and $\epsilon/k_B=402.8$ K.

After the attainment of thermal equilibrium at a temperature $T=332$ K, the dynamics of the system is followed by integrating the equations of motions with a time step $\Delta t=0.01$ ps for an overall interval of $24\,000\Delta t$. As is well known, the neutrons couple uniquely to longitudinal density fluctuations and the only way of obtaining information on transverse correlations $C_T(q,t)$ is by computer simulation. Thus we have mainly concentrated on deriving a comprehensive set of data for the latter quantity, up to times $512\Delta t$, as a starting point for the subsequent analysis leading to $n_T(q,t)$ and to the generalized viscosity $\eta(q)$. The wave vectors q were chosen of the form $(2\pi/L)(n,0,0)$, $(2\pi/L)(0,n,0)$, $(2\pi/L)(0,0,n)$, where the

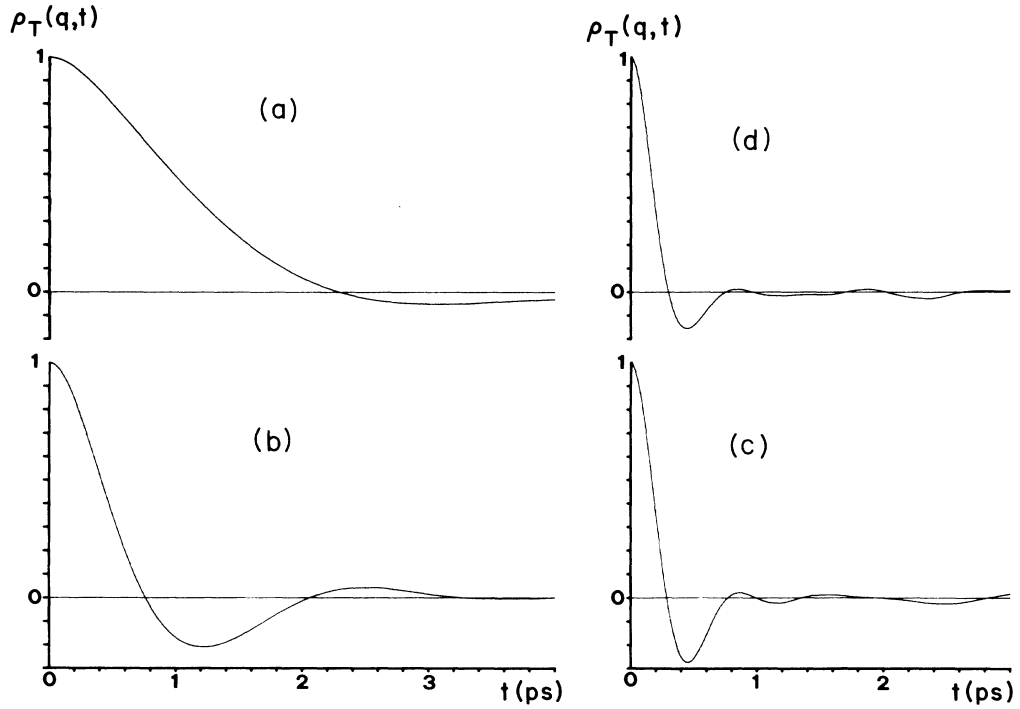

FIG. 1. Normalized transverse current correlation $\rho_T(q,t)$ in liquid rubidium at $\rho^*=0.905$, $T^*=0.824$. Wave vectors: (a) $q\sigma=0.766$, (b) $q\sigma=1.53$, (c) $q\sigma=4.594$, (d) $q\sigma=7.66$.

integer $n=1,\ldots,50$. Since for every wave vector of this form there are two independent components, for a given magnitude of $q_n=(2\pi/L)n$ the correlation $C_T(q_n,t)$ is eventually the average over six independent terms.

The results obtained for the normalized function $\rho_T(q,t)$ at several wave vectors are reported in Fig. 1. At the lowest wave vector compatible with the box length, $q_{\min}=2\pi/L$, $\rho_T(q,t)$ already shows a shallow negative minimum at long times. This contrasts with the situation in the LJ case, at a comparable wave vector, where $\rho_T(q,t)$ has a monotonic quasihydrodynamic decay.[6] Some earlier results for the liquid Rb model, by Mountain and Haan,[11]

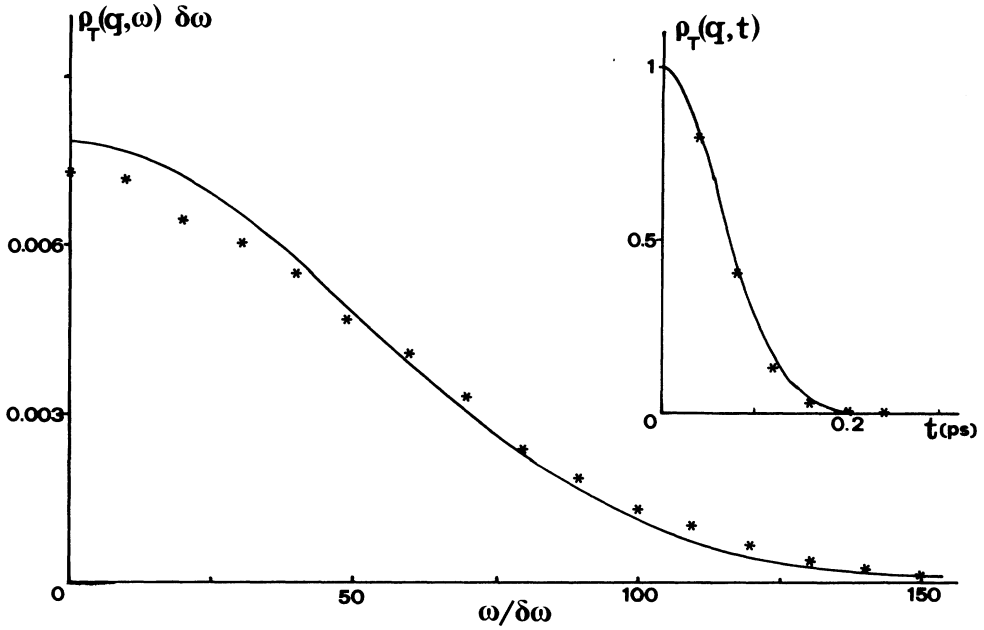

FIG. 2. Transverse current spectrum at $q\sigma=38.3$. Here and in the following figure frequencies are in units $\delta\omega=3.068\times10^{11}\ \mathrm{S}^{-1}$. The corresponding time correlation function is shown as an inset. In both cases, the stars represent the simulation data and the solid line the free-particle theoretical result.

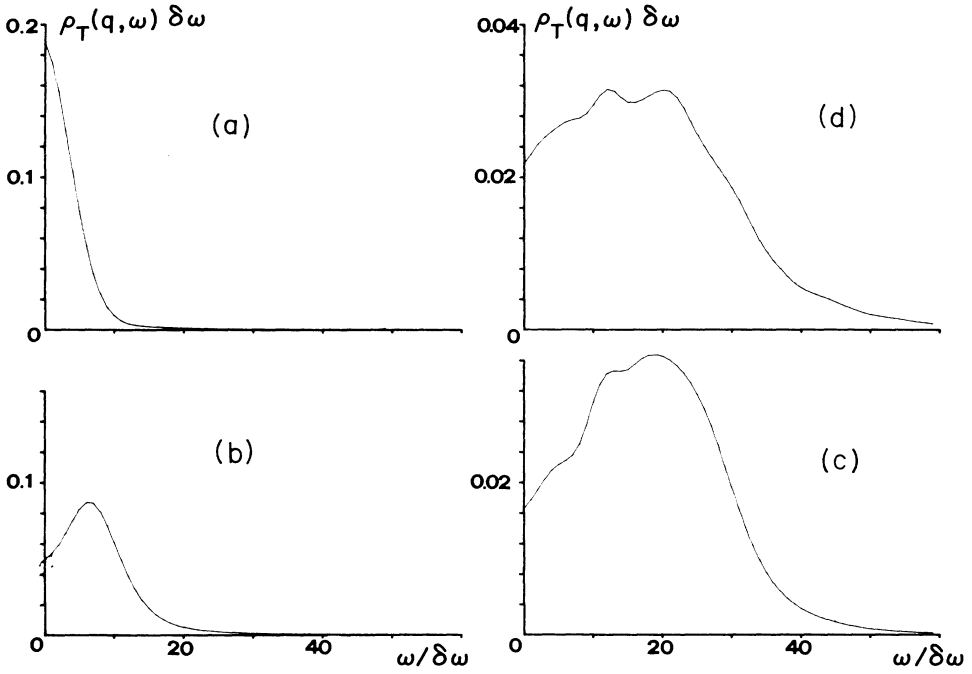

FIG. 3. Transverse current spectra $\rho_T(q,\omega)$ at the same wave vectors as in Fig. 1.

should also be mentioned here. They studied a smaller system of 250 atoms and at different thermodynamic states from the one we have selected. At a reduced density $\rho^*=0.855$ their transverse current correlation function for the smallest wave vector, $q\sigma=0.93$, appeared to show a hydrodynamiclike behavior at long times. However, the negative minimum appeared at the same wave vector when the packing fraction was increased and the temperature reduced.

As q increases, the overall time scale shrinks, the negative minimum is much more evident and an oscillatory behavior begins to appear. The last two features reach their maximum around $q\sigma\sim 4$ and gradually decrease at larger wave vectors, until eventually for $q\sigma>30$, $\rho_T(q,t)$ begins to show the structureless Gaussian decay typical of free-particle behavior (see Fig. 2). An even more evident picture of the situation is provided by the corresponding Fourier spectra

$$\rho_T(q,\omega)=(2\pi)^{-1}\int_{-\infty}^{\infty} dt\,\exp[-i\omega t]\rho_T(q,t) = \pi^{-1}\mathrm{Re}\hat{\rho}_T(q,z=i\omega) \tag{9}$$

which are reported in Figs. 2 and 3. In particular, whereas at the lowest wave vector no evidence of an inelastic peak is found, a well-defined shear wave is already apparent at $q\sigma=1.53$. This feature is clearly evident around $q\sigma=4.6$, and then gradually smears out.

Qualitatively, these features are not new; similar ones—although less pronounced—have indeed been observed both in hard spheres[12] and in the LJ liquid.[6,13] An analogous trend has also been found in *supercooled* liquid rubidium.[14]

IV. TRANSVERSE CURRENT MEMORY FUNCTION

A. Data analysis

The next quantity of our immediate interest is the memory function $n_T(q,t)$ defined in Eq. (5). As is well known, the numerical determination of a memory function from the data of the corresponding time correlation function is not straightforward. Two different methods have essentially been followed, and we shall report the results of both, together with some comments on their relative accuracy.

The first method assumes some simple analytical form for $n_T(q,t)$ containing one or more unknown parameters. The latter are determined by a least-squares fitting procedure requiring that the corresponding solution of the Mori equation

$$\dot{\rho}_T(q,t)=-(q^2/\rho m)G(q)\int_0^t d\tau\, n_T(q,t-\tau)\rho_T(q,\tau) \tag{10}$$

deviates as little as possible from the data. Since the choice of $n_T(q,t)$ is made in such a way that this solution is easily manageable, the entire procedure is relatively simple, but of course it depends on the assumed form and relies on the actual quality of the fit. Following Ref. 13, we have assumed for $n_T(q,t)$ a single-exponential (1-EXP) form

$$n_T(q,t)=\exp[-t/\tau(q)]\ , \tag{11}$$

with one parameter $\tau(q)$, as well as a more complicated 2-EXP decay

$$n_T(q,t)=(1-\alpha_q)e^{-t/\tau_{1,q}}+\alpha_q e^{-t/\tau_{2,q}}\ . \tag{12}$$

This second model reduces to the first one whenever $\alpha_q=0$ or $\tau_{1,q}=\tau_{2,q}$. In the first case the solution of Eq. (10) is analytical and reads

$$\rho_T(q,t)=e^{-t/2\tau(q)}\{\cosh[A(q)t/2\tau(q)] + [A(q)]^{-1}\sinh[A(q)t/2\tau(q)]\}\ , \quad (13)$$

where $A(q)=[1-4(q^2/\rho m)G(q)\tau(q)]^{1/2}$. Equation (13) is the well-known prediction of the viscoelastic model for the transverse current. We have already noted that within this model $\eta(q)=G(q)\tau(q)$; moreover, assuming some reasonable interpolation scheme for $\tau(q)$ (e.g., the one suggested by Akcasu and Daniels,[15]) $A(q)$ becomes purely imaginary beyond a certain wave vector and shear-wave oscillations are predicted. The 2-EXP ansatz (12) leads to a slightly more complicated result for $\rho_T(q,t)$. By substituting Eq. (12) into (10) one derives a third-order differential equation, whose characteristic equation reads

$$X^3+\left[\frac{1}{\tau_{1,q}}+\frac{1}{\tau_{2,q}}\right]X^2+\left[\frac{q^2}{\rho m}G(q)+\frac{1}{\tau_{1,q}\tau_{2,q}}\right]X + \frac{q^2}{\rho m}G(q)\left[\frac{\alpha_q}{\tau_{1,q}}+\frac{1-\alpha_q}{\tau_{2,q}}\right]=0\ . \quad (14)$$

Then

$$\rho_T(q,t)=\sum_{j=1}^{3} C_j(q)e^{\beta_j(q)t} \quad (15)$$

being $\beta_j(q)$ the solutions of (14) and $C_j(q)$ determined by the conditions $\rho_T(q,0)=1$, $\dot{\rho}_T(q,0)=0$ and $\ddot{\rho}_T(q,0)=-(q^2/\rho m)G(q)$.

The second method extracts the memory functions from the data themselves, making use of the Fourier-Laplace version of Eq. (3). Letting

$$\hat{\rho}_T(q,z=i\omega)=\rho'_T(q,\omega)+i\rho''_T(q,\omega)\ , \quad (16)$$

with

$$\rho'_T(q,\omega)=\int_0^\infty dt\cos(\omega t)\rho_T(q,t)=\pi\rho_T(q,\omega)\ , \quad (17a)$$

$$\rho''_T(q,\omega)=-\int_0^\infty dt\sin(\omega t)\rho_T(q,t)\ , \quad (17b)$$

along with similar definitions for $\hat{K}_T(q,z=i\omega)$, it is easily found that

$$K'_T(q,\omega)=(q^2/\rho m)G(q)\int_0^\infty dt\cos(\omega t)n_T(q,t) = \frac{\rho'_T(q,\omega)}{[\rho'_T(q,\omega)]^2+[\rho''_T(q,\omega)]^2}\ . \quad (18)$$

Therefore, from the data one first obtains numerically $\rho'_T(q,\omega)$ and $\rho''_T(q,\omega)$, and then $K'_T(q,\omega)$ by Eq. (18); an inverse Fourier transform finally gives $n_T(q,t)$. As far as the accuracy is concerned, the method may involve the usual complications of Fourier transforms of numerical data, such as extrapolating and smoothing effects. It has, however, the main advantage of being direct and is certainly to be preferred in all cases when the quality of the "best" fit in the first method is not very good.

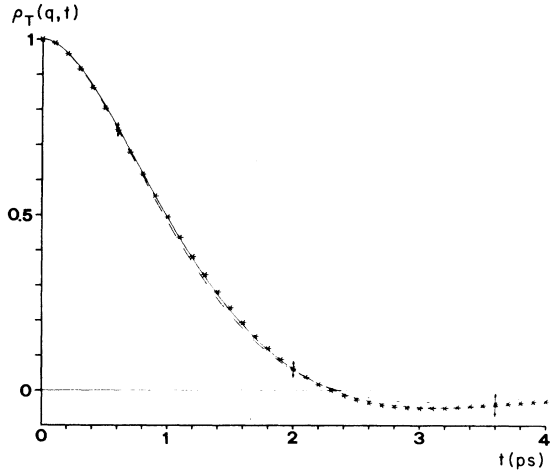

FIG. 4. Results of the fitting procedure for $\rho_T(q,t)$ in liquid rubidium at $q\sigma=0.766$. Stars: MD data. Dashed line: 1-EXP memory-function fit [parameter $\tau(q)=45.4\times10^{-14}$ s]. Solid line: 2-EXP memory-function fit (parameters $\alpha_q=0.052$, $\tau_{1,q}=40.52\times10^{-14}$ s, $\tau_{2,q}=228.5\times10^{-14}$ s). In the present and following figures an indication of the standard deviation of the MD data is given.

B. Results

The two procedures discussed so far have been applied to the previously considered data for the state $\rho^*=0.905$, $T^*=0.824$ of liquid rubidium. It is certainly interesting to compare the results with those obtained for LJ liquids and we have also made a similar analysis for these systems, using our own data at $\rho^*=0.83$, $T^*=0.79$.[6]

For both model systems the results of the 1-EXP fitting procedure are satisfactory at the smallest wave vectors, but at increasing q the quality of the fit gradually gets

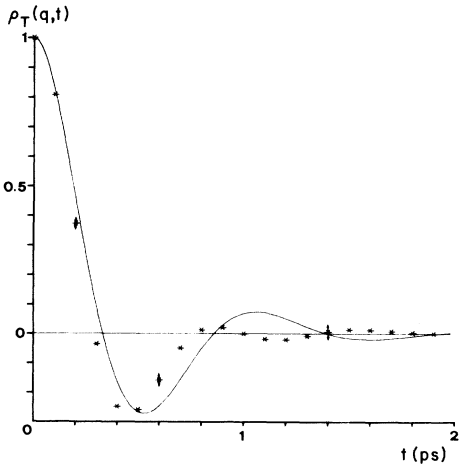

FIG. 5. Same as in Fig. 4, but at $q\sigma=4.594$. Stars: MD data. The solid line is the result of both models, 2-EXP=1-EXP. Parameters $\alpha_q=0$, $\tau(q)=20.38\times10^{-14}$ s.

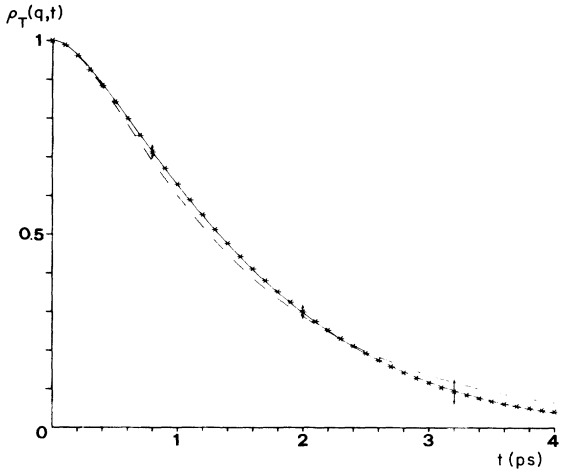

FIG. 6. Results of the fitting procedure for $\rho_T(q,t)$ in an LJ liquid ($\rho^*=0.83$, $T^*=0.79$) at $q\sigma=0.62$. Stars: MD data from Ref. 6. Dashed line: 1-EXP memory-function fit with $\tau(q)=24.9\times10^{-14}$ s. Solid line: 2-EXP memory-function fit (parameters $\alpha_q=0.114$, $\tau_{1,q}=18.4\times10^{-14}$ s, $\tau_{2,q}=84.24\times10^{-14}$ s).

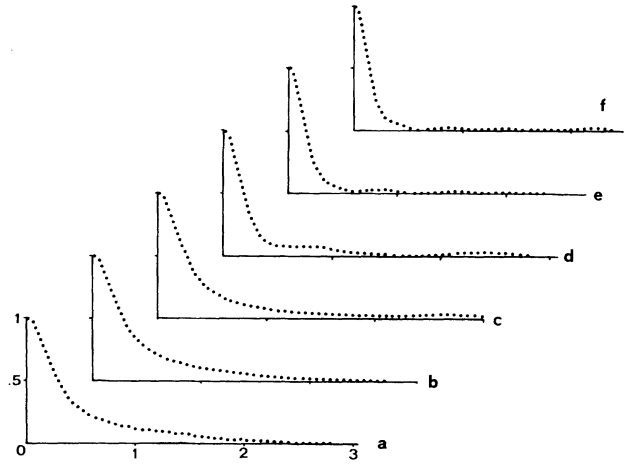

FIG. 8. Direct memory functions $n_T(q,t)$ at several wave vectors in liquid rubidium. (a) $q\sigma=0.766$, (b) $q\sigma=0.153$, (c) $q\sigma=2.30$, (d) $q\sigma=4.594$, (e) $q\sigma=6.125$, (f) $q\sigma=7.66$.

worse, the general trend being that the effect of the single exponential memory function is to overemphasize the oscillations occurring in $\rho_T(q,t)$ at intermediate wave vectors. The introduction of a second longer decay constant in the memory function (2-EXP ansatz) makes the quality of the fit better at small q, but does not improve significantly the situation in the wave-vector region where shear-wave excitations are observed. This is particularly true in the liquid metal, where beyond $q\sigma=2$ the "best" 2-EXP model is actually found to be the one with $\alpha_q=0$, thus coinciding with the 1-EXP result. Some examples illustrating this evolution at increasing wave vectors are reported in Figs. 4–7. Even in the LJ liquid at comparatively large wave vectors ($q\sigma>5$) the best 2-EXP fitting is found actually to be a single exponential, as already noticed in the early work by Levesque and Verlet.[13]

The standard physical picture behind these results is that, in general, the dynamics of the transverse current is determined by two processes (modeled by the 2-EXP ansatz) with different time scales, the shortest one being associated with binary collisional events and the longest one conventionally referred to as being due to cooperative effects, in which correlated collisions play an important role. At sufficiently large wave vectors the effects of single-particle motion gradually take over, and the second dynamical mechanism becomes progressively less important.

The relatively poor quality of the fit obtained in the

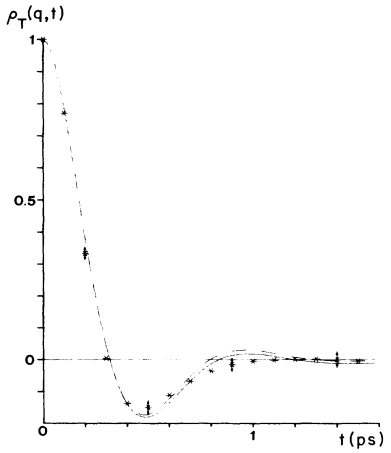

FIG. 7. Same as in Fig. 6 but at $q\sigma=3.72$. Stars: MD data from Ref. 6. Parameter of the 1-EXP memory-function fit (dashed line): $\tau(q)=13.75\times10^{-14}$ s. Parameters for the 2-EXP memory-function fit (solid line): $\alpha_q=0.015$, $\tau_{1,q}=13.37\times10^{-14}$ s, $\tau_{2,q}=32.9\times10^{-14}$s.

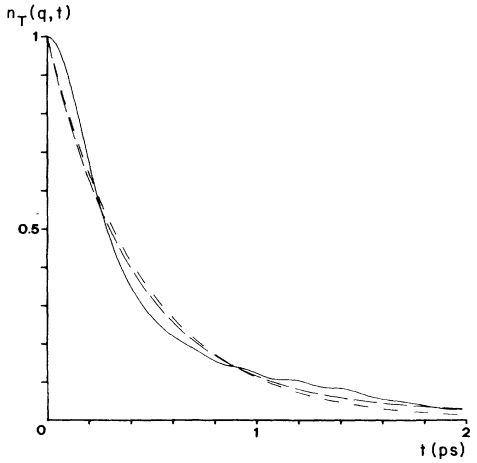

FIG. 9. Direct memory function $n_T(q,t)$ in liquid rubidium at $q\sigma=0.766$ (solid line). The dashed and the dashed-dotted lines are the 1-EXP and 2-EXP memory functions, respectively.

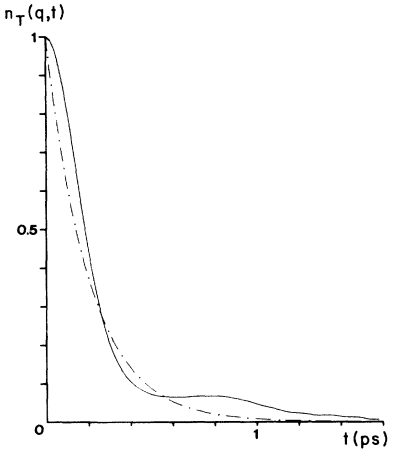

FIG. 10. Same as in Fig. 9, but at $q\sigma=4.594$. Note that in this case the fitting procedure yields 2-EXP = 1-EXP.

wave-vector region where collective transverse excitations exist, indicates that the aforementioned picture can actually be an oversimplified one. This is particularly clear if the memory functions $n_T(q,t)$, directly obtained from the data and shown for the liquid metal in Fig. 8, are compared with those derived from the fitting procedures. Such a comparison is reported in Figs. 9—12 for both model systems. In all cases there is an obvious discrepancy at short times, where both exponential models yield a finite initial slope of $n_T(q,t)$. In the above picture, this simply means that the processes involving purely binary collisions are described only in an approximate way by the models (note, however, that this inaccuracy does not have important consequences on the good quality of the fit at the lowest wave vector). Much more interesting is the situation at longer times, where collective effects become important. At the smallest wave vector for both systems, Figs. 9 and 11 show that the effective introduction of a second longer time constant provides a more adequate representation of the actual memory function in this regime. This is no longer true at larger wave vectors ($q\sigma\sim 3$—6), especially in liquid rubidium where the direct memory function exhibits a broad maximum which is clearly inconsistent with the simple two-relaxation-time picture (Fig. 10). This feature is much less pronounced in the LJ system, where beyond the binary collision regime only some extra weight in $n_T(q,t)$ is apparent, thus still giving some effective validity to the exponential fittings (see Figs. 7 and 12).

On the theoretical side, the detailed physical reasons of such a different behavior in the two systems are not clear. However, some understanding may come from the observation that at the wave vectors shown in Figs. 5 and 7, for rubidium and LJ, respectively, the dynamics of the transverse currents $\rho_T(q,t)$ is quite similar to the one probed by the velocity autocorrelation function $\psi(t) = \langle \mathbf{v}(0)\cdot\mathbf{v}(t)\rangle/\langle v^2\rangle$. Thus it is not surprising that the same intermediate-time effects previously noted in $n_T(q,t)$ at these wave vectors also appear in the memory functions associated with $\psi(t)$, as evaluated by computer simulation in LJ systems[16] and in liquid rubidium.[17] The various contributions to the dynamics of the memory function of $\psi(t)$ have been investigated by Sjögren and Sjölander[18] by a kinetic approach; in a subsequent paper, Sjögren[19] applies this analysis both to liquid Rb and to LJ systems. The consequences are that features like the broad maximum observed in the memory function in liquid Rb are largely due to couplings with density fluctuation modes. Although a similar coupling is present even in the LJ case, its magnitude is considerably reduced with respect to the liquid metal because of the larger compressibility of the latter. In the more complicated case of collective correlations the attention has mainly been focused on the density fluctuations[20] and our results may possibly stimulate a comparable theoretical understanding of transverse current correlations as well.

To close this section, let us remark that at the lowest available wave vectors the dynamical processes associated with the memory function $n_T(q,t)$ become essentially

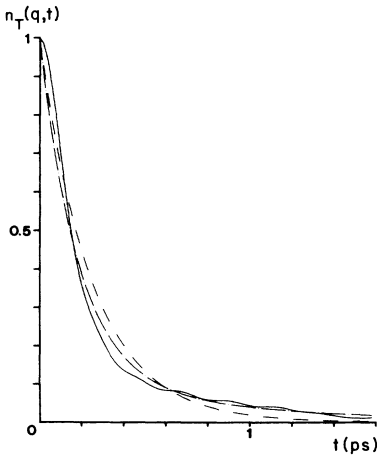

FIG. 11. Direct memory function $n_T(q,t)$ in the LJ liquid at $q\sigma=0.62$ (solid line). Dashed line: 1-EXP memory function. Dashed-dotted line: 2-EXP memory function.

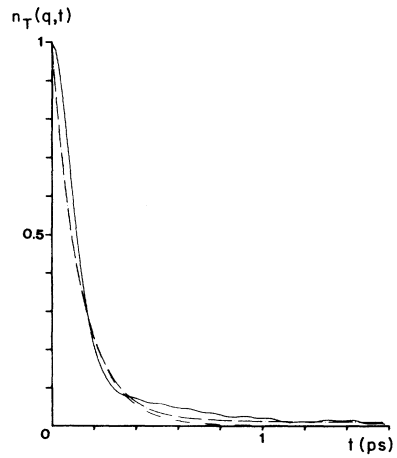

FIG. 12. The same as in Fig. 11 but at $q\sigma=3.72$.

analogous to the ones found in the stress-stress autocorrelation function. Since, strictly speaking, the latter is proportional to the memory function in the hydrodynamic $q \to 0$ limit, we expect that such an analogy is especially valid in the LJ case where the transverse current correlation at the minimum wave vector $q\sigma = 0.62$ already exhibits the long-lasting, monotonic decay typical of hydrodynamic behavior. This type of analysis, and a theoretical description in terms of various many-particle contributions to the stress-stress autocorrelation function, will be the subject of a separate paper.

V. GENERALIZED SHEAR VISCOSITY

A. Simulation data for $\eta(q)$ in liquid rubidium

As a final output of the dynamics of the transverse current it is now possible to obtain data for the generalized viscosity coefficient $\eta(q)$. As shown by Eqs. (6) or (7), $\eta(q)$ can be determined by evaluating the areas under either the memory function $n_T(q,t)$ or $\rho_T(q,t)$ itself, the two procedures being of course entirely equivalent. The results for $\eta(q)$ obtained from the direct data in liquid rubidium are reported in Fig. 13 (stars). They show a rapid fall of $\eta(q)$ in the wave-vector region where the system is able to support shear waves, followed by a slower decrease. The latter one is found to follow the q^{-1} law predicted by Eq. (8) at the largest wave vectors probed in our simulation experiment. At the other end of the explored q range, where $q\sigma = 0.766$, $\eta(q)$ turns out to be 5.17 mP, a value not very far from the estimate $\eta = 5.546$ mP for the actual viscosity coefficient at $T = 332$ K.[21]

It is interesting to compare these data with those de-

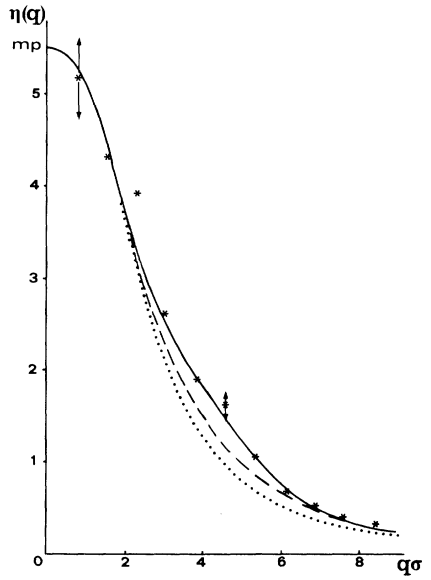

FIG. 13. Generalized shear viscosity $\eta(q)$ in liquid rubidium. Stars: MD data. Dotted line: viscoelastic model $\eta(q) = G(q)\tau(q)$ with $\tau(q)$ determined according to the Akcasu and Daniels prescription, Eq. (19), with $\eta = 5.5$ mP. Dashed line: results from the 2-EXP memory-function fit. Solid line: results of the modified viscoelastic model, Eq. (22). Typical statistical errors (of the order of 10%) are reported over some MD results.

duced from the 2-EXP assumption for the memory function. Such a comparison is also reported in Fig. 13 together with the viscoelastic 1-EXP result $\eta(q) = G(q)\tau(q)$, where, rather than by a fitting procedure, $\tau(q)$ is determined by the interpolation formula of Akcasu and Daniels[15]

$$\tau(q) = \left[2\frac{q^2 G(q)}{\rho m} + \frac{[G(0)/\eta]^2 + 2(q^2/\rho m)[G(q) - \rho k_B T]}{1 + (q/q_0)^2} \right]^{-1/2}, \tag{19}$$

where q_0 is given a value close to the wave vector where the static structure factor has its principal maximum (we choose $q_0\sigma = 6.23$ in liquid rubidium). The agreement between these different models is seen to be fairly good, but neither one is able to account for the data in the wave-vector range $2 < q\sigma < 8$, where the direct $\eta(q)$ is found to be distinctly larger. The appearance of this "shoulder" in the generalized viscosity has already been noted in the LJ case,[6] in which, however, the effect is less pronounced. Recalling the main results obtained in Sec. IV, the presence of the shoulder can be traced back to the increased amplitude of the actual memory function at intermediate and long times (see Fig. 10).

B. Microscopic version of the Stokes-Einstein law for the self-diffusion coefficient D

The extension of the concept of velocity field down to microscopic distances has led to theoretical results for the velocity autocorrelation function of a single particle[2] as well as for the cross correlation which describes the transfer of momentum from a central atom to its neighbors.[21,22] In both cases a satisfactory agreement with the respective simulation data has been found. One of the consequences of this approach is a microscopic generalization of the Stokes-Einstein law for the self-diffusion coefficient,

$$D_H = k_B T/(4\pi\eta R), \tag{20}$$

where R is the particle "radius" and slip boundary conditions have been assumed. Equation (20) is expected to be rigorous for a Brownian particle immersed in a continuous medium with viscosity η, i.e., for a situation where the separation of length and time scales, typical of hydrodynamics, is certainly valid. The proper generalization of Eq. (20) reads[4]

$$D=\frac{k_B T}{4\pi}\frac{4\rho}{3\pi}\int_0^\infty dq\frac{f(q)}{\eta(q)}\ , \tag{21}$$

where $f(q)=4\pi a^2 j_1(qa)/q$ and the length a is determined by $\frac{4}{3}\pi\rho a^3=1$. If the wave-vector dependence of $\eta(q)$ is ignored (the generalized viscosity being approximated by its hydrodynamic value η), one retrieves Eq. (20) with the quantity a playing the role of the particle radius. Although the latter approximation gives reasonable results for the diffusion coefficient, it is found that D is generally underestimated by an amount ~ 25–30%. Since clearly the approximation $\eta(q)\sim\eta$ is unrealistic in the whole wave-vector range, a significant improvement is expected by taking into account the strong decrease of the generalized viscosity $\eta(q)$. Indeed, in LJ "argon" where $D=2.39\times10^{-5}$ cm^{2}s^{-1},[4] the hydrodynamic value is found to be substantially lower ($D_H=1.70\times10^{-5}$ cm^{2}s^{-1}), whereas excellent agreement is obtained by using the viscoelastic result with $\tau(q)$ given by Eq. (19) ($D=2.34\times10^{-5}$ cm^{2}s^{-1}). This success is to some extent fortunate, since the integral in Eq. (21) is very sensitive to the details of $\eta(q)$ and the effects of the small shoulder, which is absent in the viscoelastic model, are practically cancelled by those coming from other minor discrepancies at larger wave vectors.[6]

In liquid rubidium, taking $\eta=5.5$ mP, the hydrodynamic prediction for the diffusion coefficient turns out to be $D=2.35\times10^{-5}$ cm^{2}s^{-1}, somewhat lower than the observed value $D=2.66\times10^{-5}$ cm^{2}s^{-1}.[21] If the decrease of $\eta(q)$ is approximately taken into account by the simplest viscoelastic prescription $G(q)\tau(q)$—Eqs. (4′) and (19)—one finds a substantial overestimate of the diffusion coefficient, $D=3.84\times10^{-5}$ cm^{2}s^{-1}. Clearly the fortunate cancellation found in the LJ case is not effective in the liquid metal, and this discrepancy is mainly due to the neglect of the pronounced shoulder in $\eta(q)$, around $q\sigma\sim4$, when compared with the viscoelastic prediction $[\eta(q)]_{\rm VE}$ (Fig. 13). This shoulder effect can be taken into account in a phenomenological way, for example letting

$$\eta(q)=[\eta(q)]_{\rm VE}+A(q/q_1)^n e^{-n[(q/q_1)-1]}\ . \tag{22}$$

Figure 13 shows that the choice $A=0.55$ mP, $q_1\sigma=4$, $n=9$ provides a satisfactory description of the observed q dependence of $\eta(q)$ even in the intermediate wave-vector range. If the modified expression (22) is now used to evaluate the diffusion coefficient according to Eq. (21), one finds $D=2.73\times10^{-5}$ cm^{2}s^{-1}. The very good agreement with the MD value confirms the relevance of the increased magnitude of $\eta(q)$ in the intermediate wave-vector range. The structure in the data at $q\sigma\sim2.3$, which is not described by Eq. (22), has a much smaller effect on D. Estimates suggest that it will produce a further reduction by a few percent.

VI. CONCLUSIONS

In this paper we have addressed three main points. The first one regards the specific features of the transverse current memory function at several wave vectors. The usual phenomenological models were found to be insufficient to reproduce the actual dynamics of the transverse current correlation, particularly in the wave-vector range where shear-wave oscillations are more easily supported. The different behavior of a model simulating liquid rubidium with respect to the LJ system was discussed and some arguments which might be useful for a full theoretical explanation were raised.

The second point, partly related to the first one, concerns the wave-vector dependence of the corresponding transport property, namely, the generalized shear viscosity coefficient $\eta(q)$. It shows a rapid decrease eventually followed by a q^{-1} behavior typical of the free-particle regime. In the interesting transition region between hydrodynamics and kinetic regime a shoulder appears which turns out to be more pronounced in liquid rubidium than in the LJ system.

The consequences of this behavior have been analyzed in discussing the third point of our work, namely, the microscopic generalization of the Stokes-Einstein relation between the self-diffusion coefficient and generalized shear viscosity. The presence of the shoulder in $\eta(q)$ is found to be of relevance in reproducing the proper value of the diffusion coefficient in the metallike system investigated in this paper.

ACKNOWLEDGMENTS

This work has been partially supported by the North Atlantic Treaty Organization (NATO) Scientific Affairs Division (Grant No. 040/84). Computing time at Centro di Calcolo Elettronico Interuniversitario dell'Italia Nord-Orientale (CINECA, Bologna, Italy) was made available through a Consiglio Nazionale delle Ricerche (CNR) convention.

[1] J. P. Boon and S. Yip, *Molecular Hydrodynamics* (McGraw-Hill, New York, 1980). For a recent review, see also A. Sjölander, in *Amorphous and Liquid Materials (Trento, 1985), NATO Advanced Institute Series B* (Plenum, New York, in press).

[2] T. Gaskell and S. Miller, J. Phys. C **11**, 3749 (1978).

[3] H. Hahn and M. Matzke, Physikalisch Technische Bundesanstalt, Braunschweig Report No. PTB-FMRB-105 (1984) (unpublished).

[4] U. Balucani, R. Vallauri, T. Gaskell, and M. Gori, J. Phys. C **18**, 3133 (1985).

[5] W. E. Alley and B. J. Alder, Phys. Rev. A **27**, 3158 (1983).

[6] T. Gaskell, U. Balucani, M. Gori, and R. Vallauri, Physica Scr. **35**, 37 (1987).

[7] K. E. Larson and W. Gudowski, Phys. Rev. A **33**, 1968 (1986).

[8] D. L. Price, K. S. Singwi, and M. P. Tosi, Phys. Rev. B **2**, 2983 (1970).

[9] A. Rahman, Phys. Rev. Lett. **32**, 52 (1974); Phys. Rev. A **9**, 1667 (1974). Recently the adequency of the potential of Price *et al.* in predicting also the shear viscosity coefficient has been demonstrated by P. T. Cummings and G. P. Morris, J. Phys. F (to be published).

[10]J. W. E. Lewis and S. W. Lovesey, J. Phys. C **10**, 3221 (1977); **11**, L57 (1978).
[11]R. D. Mountain and S. W. Haan, J. Res. Nat. Bur. Stand. **84**, 439 (1979).
[12]W. E. Alley, B. J. Alder, and S. Yip, Phys. Rev. A **27**, 3174 (1983).
[13]D. Levesque, L. Verlet, and J. Kurkijárvi, Phys. Rev. A **7**, 1690 (1973).
[14]R. D. Mountain, Phys. Rev. A **26**, 2859 (1982).
[15]A. Z. Akcasu and E. Daniels, Phys. Rev. A **2**, 962 (1970).
[16]D. Levesque and L. Verlet, Phys. Rev. A **2**, 2514 (1970).
[17]A. Rahman [unpublished results reported in L. Sjögren and A. Sjölander, J. Phys. C **12**, 4369 (1979)].
[18]L. Sjögren and A. Sjölander, J. Phys. C **12**, 4369 (1979).
[19]L. Sjögren, J. Phys. C **13**, 705 (1980).
[20]L. Sjögren, Phys. Rev. A **22**, 2866 (1980); **22**, 2883 (1980). In the LJ case the results of a mode-coupling analysis, also involving the transverse case, have been reported by J. Bosse, W. Götze, and M. Lucke, Phys. Rev. **17**, 447 (1978).
[21]U. Balucani, R. Vallauri, T. Gaskell, and M. Gori, Phys. Lett. **102A**, 109 (1984).
[22]U. Balucani, R. Vallauri, C. S. Murthy, T. Gaskell, and M. S. Woolfson, J. Phys. C **16**, 5605 (1983).